Available online at www.sciencedirect.com
ScienceDirect
Journal of Colloid and Interface Science 320 (2008) 177–185
JOURNAL OF Colloid and Interface Science
www.elsevier.com/locate/jcis

# An ATR-FTIR spectroscopic approach for measuring rapid kinetics at the mineral/water interface

S.J. Parikh *, B.J. Lafferty, D.L. Sparks

*Department of Plant and Soil Sciences, Center for Critical Zone Research, The University of Delaware, 152 Townsend Hall, Newark, DE 19716, USA*

Received 28 September 2007; accepted 4 December 2007

Available online 23 December 2007

**Abstract**

This study presents a methodology for studying rapid kinetic reactions for IR active compounds. In soils, sediments, and groundwater systems a rapid initial chemical reaction can comprise a substantial portion of the total reaction process at the mineral/water interface. Rapid-scan attenuated total reflectance (ATR) Fourier transform infrared (FTIR) spectroscopy is presented here as a new method for collecting rapid *in situ* kinetic data. As an example of its application, the initial oxidation of arsenite ($As^{III}$) via Mn-oxides is examined. Using a rapid-scan technique, IR spectra were collected with a time resolution of up to 2.55 s (24 scans, 8 $cm^{-1}$ resolution). Through observation and analysis of IR bands corresponding to arsenate ($As^{V}$), rapid chemically-controlled $As^{III}$ oxidation is observed (initial pH 6–9) with 50% of the reaction occurring within the first one min. The oxidation of $As^{III}$ is followed by rapid binding of $As^{V}$ to HMO, at least in part, through surface bound $Mn^{II}$. The experimental data indicate that rapid-scan FTIR is an effective technique for acquisition of kinetic data, providing molecular scale information for rapid reactions at the solid/liquid interface.


*Keywords:* ATR-FTIR; Rapid kinetics; Mn-oxide; Arsenic

## 1. Introduction

In soil and aquatic environments, chemical reactions at the mineral/water interface take place over a range of temporal scales, ranging from microseconds to years [1]. Many important processes (e.g., adsorption, oxidation–reduction) occur on natural sorbents, such as clay minerals, metal hydr(oxides) and soils, and are characterized by a rapid initial reaction on a time scale of seconds to minutes [2,3]. Knowledge of these initial rates is critical to determine rate constants and elucidate reaction mechanisms, both of which are necessary for understanding rapid chemical processes [4]. Rapid kinetic measurements of reaction rates are typically limited by experimental techniques that yield relatively few data points during the initial reaction period. These reactions cannot be accurately determined using traditional batch and flow techniques and, accordingly, there exists a need for experimental techniques to collect rapid kinetic data at the mineral/water interface [5].

Many difficulties encountered when monitoring reaction kinetics on mineral surfaces result from analytical challenges in measuring concentrations in suspensions. Rapid measurement of solution phase species (e.g., heavy metals, organic contaminants) can be readily accomplished; however, filtration to remove the solid phase is time consuming and greatly reduces temporal resolution. Likewise, solid phase extraction to determine bound species is laborious and time intensive. *In situ* experiments are required to monitor kinetic reactions of suspensions without separation. Ion selective electrodes and limited spectroscopic techniques can be used to monitor reaction kinetics at the solid/liquid interface [1]. For example, quick X-ray absorption fine structure (XAFS) spectroscopy has been used to study arsenic (As) oxidation on amorphous Mn-oxide using a column reactor with data acquisition at 1 min intervals [6]. Additionally, attenuated total reflectance (ATR) Fourier transform infrared (FTIR) was used to monitor the oxidation of $As^{III}$ by hydrogen peroxide on a ferrihydrite surface with a time resolution of 2 min [7].

* Corresponding author.
*E-mail address:* sjparikh@udel.edu (S.J. Parikh).

0021-9797/$ – see front matter 
doi:10.1016/j.jcis.2007.12.017

ATR-FTIR is an established technique for studying sorption [8,9] and redox [7,10] processes, providing bonding mechanisms and, under certain reaction conditions, kinetic data. ATR-FTIR is a useful technique for biogeochemical applications as it probes the mineral/liquid interface, providing information for solid and solution phase species. Through observing shifts in IR peak location and formation of new IR peaks, sorption and/or formation of reaction products can be ascertained. In this study, we present the use of rapid-scan ATR-FTIR to monitor chemical reaction processes for IR active compounds at the mineral/liquid interface on a temporal resolution of 2.55 s. To demonstrate this technique the *in situ* rapid oxidation of $As^{III}$ via Mn-oxides is studied.

Due to the environmental and human health risks associated with both natural and anthropogenic As in soils and sediments, an increased understanding of As oxidation reactions with Mn-oxides is required. The general term Mn-oxides refers to manganese oxide/hydroxide minerals containing $Mn^{IV}$, but some contributions of $Mn^{III}$ are often also present. Kinetic investigations of $As^{III}$ oxidation reactions with Mn-oxides have revealed relatively fast $As^{III}$ depletion rates [11–13], with equilibrium reached on a time scale of minutes to hours. However, the time resolution of previous studies does not permit examination of initial reaction rates, potentially missing important information within the first minute of reaction. Additionally, in previous studies, $As^{III}$ and $As^{V}$ in solution or extracted from the solid phase were measured to determine the rate and extent of reaction. Kinetic rates derived from measurements of solution phase $As^{III}$ and $As^{V}$ are influenced by sorption processes; therefore, aqueous As concentrations do not reflect the total amount of As present. The retention of $As^{V}$ to Mn-oxides surfaces subsequent to $As^{III}$ oxidation, likely via bridged mineral-bound $Mn^{II}$, has been documented [11,12]. For these reasons the use of a technique, such as ATR-FTIR, that probes the solid–liquid interface is desirable. To our knowledge the only study investigating the Mn-oxide/liquid interface during $As^{III}$ oxidation was conducted by Mitsunobu et al. [6] using quick XAFS. However, in that study, data was collected at 1 min intervals and the first 12 min of reaction were not included in data interpretations.

The primary aim of this research is to present a new technique for monitoring rapid kinetic reactions of IR active compounds. To demonstrate the technique we present data on the rapid oxidation of $As^{III}$ on birnessite and hydrous manganese oxide (HMO), a poorly crystalline Mn-oxide similar to birnessite [14]. The data illustrate the effectiveness of rapid-scan FTIR to obtain kinetic data at the molecular level for both static and flow conditions. To our knowledge, this is the first study to apply rapid-scan ATR-FTIR to monitor rapid geochemical reactions at the mineral/water interface.

## 2. Experimental procedures

### 2.1. Materials

HMO synthesis was carried out via standard methods [15]. Following synthesis, it was washed with Barnstead Nanopure (BNP) water via centrifugation (3000 RCF, 20 min) three times and dialyzed (Spectra/Por, 12,000–14,000 MWCO, Spectrum) against BNP water until the electrical conductivity remained unchanged for a 12 h period. The HMO was stored at 4 °C for ∼9 months prior to use in experiments. Prior to use, HMO was centrifuged at 10,000 RCF for 20 min and supernatant discarded to remove small particles. This method of HMO synthesis yields $MnO_x$, with $x$ ranging from 1.90 to 1.95 [14] and a point of zero charge (PZC) of 2.4 [14,16]. HMO suspension concentration was determined by drying an aliquot of suspension and measuring the residual mass. The BET surface area for air-dried HMO, determined via multi-point $N_2$ adsorption (Tristar 3000, Micromeritics) with remaining adsorbed water removed during BET procedure.

Birnessite ($\delta$-$MnO_2$) was provided from the laboratory of Dr. Jon Chorover at The University of Arizona. Synthesis involves adding concentrated HCl to a boiling solution of $KMnO_4$ [17]. Birnessite was washed via centrifugation with 1 mmol $kg^{-1}$ HCl followed by BNP water until $Cl^{-1}$ was no longer measured and the sample was freeze-dried. This birnessite had a BET surface area of 83.8 $m^2\,g^{-1}$ [18]. The PZC of birnessite ranges from 1.5 to 2.5 [19].

All solutions were prepared in acid-washed glass bottles using BNP water in a background electrolyte solution of 1 mmol $kg^{-1}$ NaCl with pH adjustment via addition of NaOH/HCl. Sodium arsenite ($Na_2AsO_2$; Fischer Scientific, >99% pure) and sodium hydrogen arsenate heptahydrate ($Na_2HAsO_4{\cdot}7H_2O$; Alfa Aesar, 98–102% pure) were used as sources of $As^{III}$ and $As^{V}$, respectively. Stock $As^{III}$ and $As^{V}$ solutions were pH adjusted to 6, 7, 8, and 9. All solutions were pre-equilibrated overnight at 4 °C in the dark, brought to room temperature, and the pH checked before use.

Stock mineral solutions were made in polypropylene vials with a background electrolyte solution of 1 mmol $kg^{-1}$ NaCl with pH adjustment via addition of NaOH/HCl. Adjustment of pH for HMO and birnessite suspensions required equilibrating and readjusting pH for several days. Stock mineral suspensions (HMO: 60 g $kg^{-1}$, birnessite: 106 g $kg^{-1}$) allow for equal volumes of reactants to be used in experiments with a constant mineral surface area (8.90 $m^2\,g^{-1}$).

### 2.2. ATR-FTIR spectroscopy and analysis

All FTIR spectra were collected with a Thermo Nicolet Nexus spectrometer (Thermo) using single bounce ATR-FTIR spectroscopy (Smart Orbit, Thermo) with a diamond internal reflection element (IRE) at ambient temperature (23 ± 1 °C). Spectra were collected using standard spectral collection techniques and the rapid-scan software in Omnic 7.0 (Thermo). In all cases spectra were collected using 24 scans at 8 $cm^{-1}$ and a MCT/A detector. A minimum of duplicate experiments/spectra were collected to verify reproducibility of results. Peak areas for $As^{V}$ were determined using Omnic 7.0 by integrating from 794 to 944 $cm^{-1}$. All spectra were collected with background spectra acquired using a 1 mmol $kg^{-1}$ NaCl solution at the appropriate pH prior to each experiment.

Spectra of $As^{III}$ and $As^{V}$ were collected to determine detection limits and to verify our ability to distinguish between

the two arsenic species. Spectra were collected for 100 μL of $As^{III}$ or $As^{V}$ solutions, that were deposited on the diamond IRE, at varying pH. Peak locations for $As^{III}$ and $As^{V}$, as a function of pH, were also verified. Peak areas of $As^{V}$, as a function of concentration and pH, were calculated to create a calibration curve used to determine final concentrations of $As^{V}$ produced via $As^{III}$ oxidation (Table S1).

$As^{V}$ solutions were independently reacted with HMO and birnessite to determine peak locations for $As^{V}$–Mn-oxide systems as a function of pH. A 100 μL aliquot of 50 mmol $kg^{-1}$ $As^{V}$ was reacted with 100 μL HMO and birnessite suspensions (surface area = 4.45 $m^2$ $g^{-1}$) for 10 min on the diamond IRE and spectra collected (pH 6–9).

The location and splitting of $As^{V}$ IR peaks is pH dependent, and therefore quantification of $As^{V}$ concentration is challenging. Careful calibration of $As^{V}$–Mn-oxides as a function of pH permits calculation of product concentrations for the final pH. Due to the rapid reaction rate real-time measurement of pH values during reaction are not possible. Resulting, $As^{V}$ concentrations are presented only for final pH values to reflect the amount of $As^{V}$ present at the end of the experiment. IR peak areas are used for kinetic plots where accurate concentrations cannot be calculated. Due to these constraints, the data collected in this study are quantified using a conservative approach for comparing data. For static experiments, the maximum amount of $As^{V}$ produced ($As^{V}_{max}$) is estimated by calculating the mean for all data points from 4 to 20 min, representing near completion of the reaction. Under flow conditions, $As^{V}_{max}$ is determined by the maximum $As^{V}$ peak area obtained over the course of the reaction. The amount of time required for half $As^{V}_{max}$ to be produced is defined as $t_{1/2}$. Additionally, linear regression analysis (peak area vs time) was used to determine the slope of the first 30 s of reaction ($m_{30\,s}$) for comparison of initial reaction rates.

### 2.3. In situ static FTIR experiments

Rapid-scan FTIR spectra of $As^{III}$ oxidation were acquired every 2.55 s using the collection parameters previously described. To verify accuracy of spectra collected via rapid-scan, additional spectra were collected using standard collection techniques with a 12 s time resolution. Although spectral collection parameters are identical under the two collection methods the acquisition of data differs in the speed of the moving mirror within the interferometer. In rapid-scan mode the mirror does not stop moving and processing of data is carried out upon completion of the experiment. This technique does not permit mirror settling time, and therefore minor noise in the data is expected. Under standard collection parameters spectral quality is somewhat increased; the moving mirror stops briefly after each scan, and thus data cannot be collected as quickly.

Investigations were carried out at 25, 50, and 75 mmol $kg^{-1}$ $As^{III}$ with an electrolyte background of 1 mmol $kg^{-1}$ NaCl at pH values of 6, 7, 8, and 9. The $As^{III}$ solution was deposited on the IRE (100 μL) and spectra collected for 2 min; addition of 100 μL HMO or birnessite at 2 min indicates $t = 0$ for the $As^{III}$ oxidation reaction. A Teflon cover was placed over the slurry to prevent evaporation. The addition of a high concentration of Mn-oxide to a small volume of $As^{III}$ solution at the IRE interface allows for rapid mixing of the solid and solution. Spectral acquisition of $As^{III}$ reaction with Mn-oxides was collected for 20 min. Additional *in situ* experiments were conducted to collect data at longer time intervals. The slurry temperature increased approximately 0.1 °C upon addition of HMO within 10 s of reaction and slowly drifted back to ambient temperature (∼10 min) over the course of the experiment.

To check the accuracy of this method, which requires complete mixing and no preferential accumulation of $As^{V}$ at the crystal interface, exploratory investigations were carried out with continuous mixing of the HMO/$As^{III}$ slurry over the entire reaction time. Stirring was achieved by manually moving a plastic pipette tip back and forth over the diamond IRE for the duration of the experiment. Additionally batch *ex situ* reactions were carried out by pipetting 100 μL aliquots from a glass vial containing the HMO-$As^{III}$ suspension onto the IRE at several reaction times.

To determine sorption of $As^{V}$ to HMO, *ex situ* batch reactions (200 μL; 75 mmol $kg^{-1}$ $As^{III}$, 30 g $L^{-1}$ HMO) were syringe filtered (0.2 μm) and washed with 1 mL of either 5 mM NaCl or $CaCl_2$. The filtrate, filtered mineral paste, and washed mineral paste were deposited on the diamond IRE and spectra collected with 128 coaveraged scans at 4 $cm^{-1}$ resolution. Spectra were processed with a diamond IRE background and the appropriate spectra of NaCl, $CaCl_2$, HMO slurry, or HMO mineral paste were subtracted.

### 2.4. In situ flow experiments

A stainless steel flow chamber (30 μL) was used to collect FTIR spectra in real time with a flow rate of 20 μL $min^{-1}$. A preequilibrated aliquot of 20 μL (pH 6 and 9, 1 mmol $kg^{-1}$ NaCl) HMO stock suspension was placed in the chamber. A 0.45 μm HV Durapore membrane filter was placed between the IRE and inlet/outlet to prevent solid material from exiting the chamber. A 1 mmol $kg^{-1}$ NaCl solution (pH 6 and 9) was pumped through the flow cell and background spectra acquired. Spectra collection was initiated 2 min prior to addition of 75 mmol $kg^{-1}$ $As^{III}$ solution (pH 6 and 9) to the flow cell at a rate of 1 mL $min^{-1}$ (for 2 s), for near immediate addition of 75 mmol $kg^{-1}$ $As^{III}$ to the flow chamber. The flow rate was swiftly reduced to 20 μL $min^{-1}$ for the 40 min reaction period examined. Spectra were collected using previously mentioned parameters at 12 s intervals.

## 3. Results

### 3.1. FTIR spectra of $As^{III}$ and $As^{V}$ standards

Using the current ATR-FTIR technique $As^{V}$ at pH 6 is readily detected from approximately 7 mmol $kg^{-1}$ to concentrations greater than 500 mmol $kg^{-1}$; IR absorbance increases with increasing pH. $As^{III}$ peaks are much smaller and often difficult to detect, particularly at low pH. A small IR peak for a 100 mmol $kg^{-1}$ $As^{III}$ solution at pH 9 is observed at

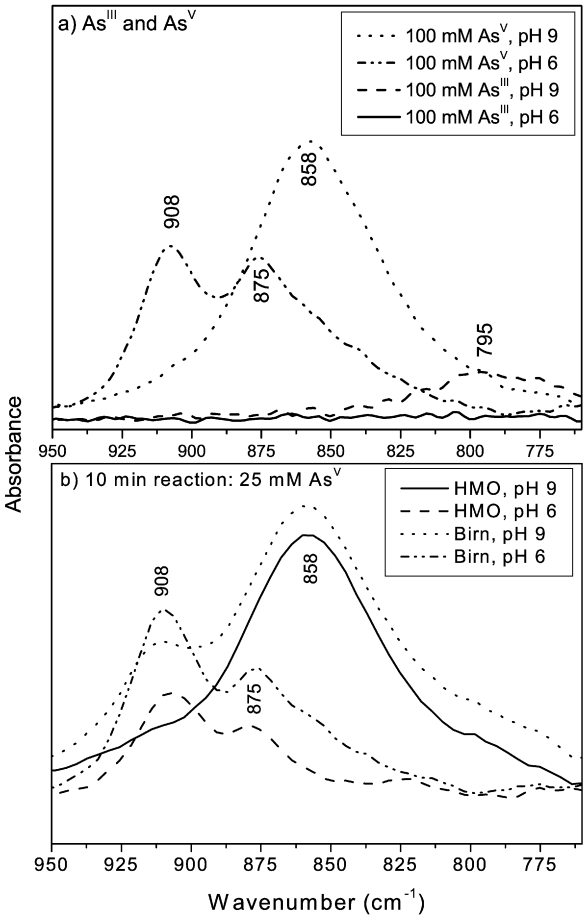


Fig. 1. ATR-FTIR spectra of (a) As$^{III}$ and As$^{V}$ standards showing at pH 6 and 9 and (b) spectra resulting from 10 min reaction of As$^{V}$ to HMO and birnessite.

795 cm$^{-1}$ [$\nu$(As–O)]; no peak is observed when the pH is reduced to 6 (Fig. 1a). Solutions of 100 mmol kg$^{-1}$ As$^{V}$ produce strong IR bands at both pH 9 [858 cm$^{-1}$: $\nu_{as}$(As–O)] and pH 6 [875 cm$^{-1}$: $\nu_{s}$(As–O); 908 cm$^{-1}$: $\nu_{as}$(As–O)], in agreement with reported values [20,21]. The shift and splitting of As$^{V}$ peaks resulting from functional group protonation are observed with decreasing pH (Fig. 1a). Spectra from reaction of As$^{V}$ with birnessite and HMO (Fig. 1b) are similar to samples at the same pH with no mineral phase present (Fig. 1a), with As$^{V}$ IR peaks slightly larger upon reaction with birnessite. Both suspension and solution pH remain unchanged after 20 min reaction of As$^{V}$ with HMO and birnessite.

### 3.2. *In situ static FTIR experiments*

Collection of kinetic IR data without mixing on the IRE (static), with mixing on the IRE, and via *ex situ* batch give near identical As$^{V}$ peak areas as a function of reaction time for As$^{III}$ oxidation via HMO (Fig. 2). These data verify that the reaction suspensions during *in situ* static kinetic experiments are well mixed and that particle settling does not influence the acquired spectra. Additionally, due to varied duration of samples absorbing evanescent IR light (*ex situ* vs *in situ*) the data confirm minimal effect of thermal absorption from the IR beam on

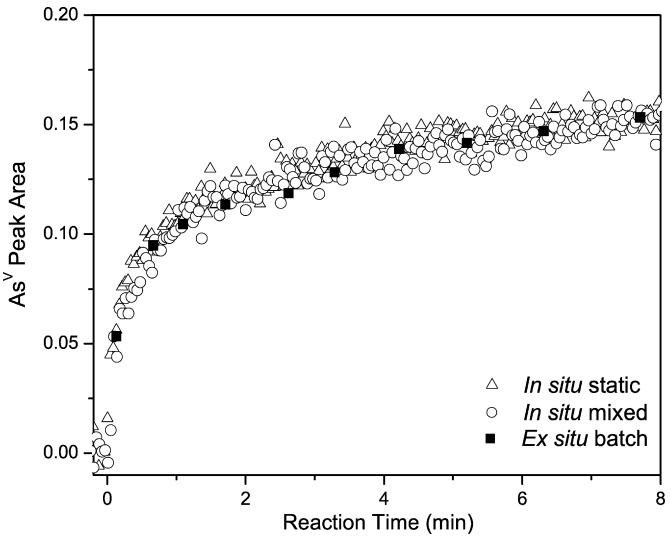


Fig. 2. Kinetic data collected via rapid-scan ATR-FTIR spectroscopy using different sample mixing and settling parameters.

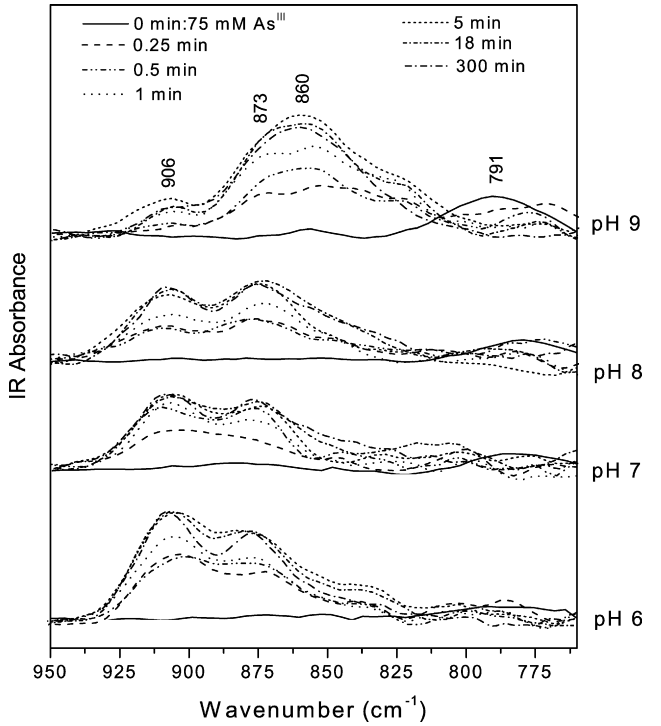


Fig. 3. ATR-FTIR spectra for HMO reacted with 75 mmol kg$^{-1}$ As$^{III}$ at pH 6, 7, 8, and 9. Within 1 min of reaction As$^{V}$ peaks (860, 873, 906 cm$^{-1}$) are observed and only minimal changes in spectra are observed in a subsequent 300 min period.

samples and corresponding spectra during the course of the experiment.

Prior to reaction, small As$^{III}$ peaks are observed in the spectra. After HMO addition to the As$^{III}$ solution, strong IR peaks at 860 cm$^{-1}$ [$\nu_{s}$(As–O)], 873 [$\nu_{s}$(As–O)], and 906 cm$^{-1}$ [$\nu_{as}$(As–O)] of As$^{V}$ are observed within 1 min for all pH values examined (Fig. 3). Spectra for times >1 min are similar with slight variation in peak intensities. After addition of HMO or birnessite, immediate production of As$^{V}$ is observed and the reac-

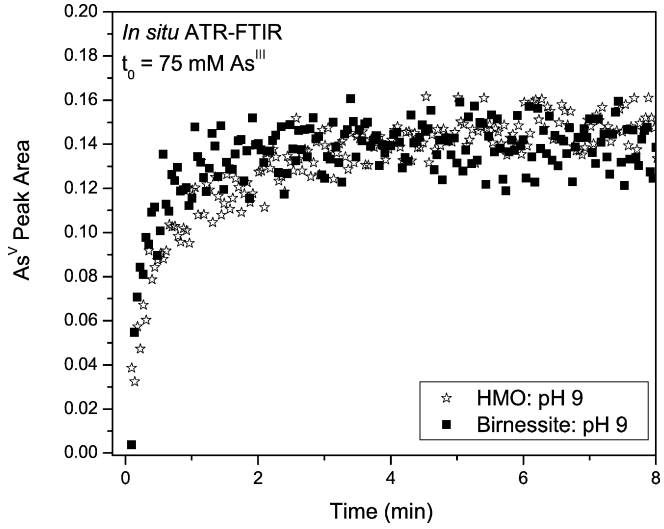


Fig. 4. *In situ* ATR-FTIR kinetic measurements showing $As^V$ production via oxidation of 75 mmol $kg^{-1}$ $As^{III}$ via HMO and Birnessite at pH 9.

tion nears completion at ∼4 min, followed by a slight increase in $As^V$ peak area, particularly for higher $As^{III}$ concentrations (Figs. 4 and 5). Surface passivation by reaction products or precipitation, particularly for higher initial concentrations, prevent all $As^{III}$ from being oxidized to $As^V$ and therefore "completion" of reaction refers to the point at which $As^V$ is no longer produced. Data for $As^{III}$ oxidation via HMO over pH and concentration ranges (Fig. 5), also reveal rapid $As^{III}$ oxidation with $t_{1/2} < 1$ min for all reactions (Table 1). Experiments with both higher (8.9 $m^2\,g^{-1}$) and lower (2.23 and 1.48 $m^2\,g^{-1}$) HMO surface area (data not shown) reveal similar rapid reaction with $As^V$ peak intensity remaining constant as the reaction rate slows and nears completion. Increasing the HMO surface area does result in increased final concentrations of $As^V$.

A decrease in pH was observed within the initial 20 min reaction for all initial pH values (9 to 7.5, 8 to 6.5, 7 to 5.85, and 6 to 5.5); initial pH values are used for discussion of results. The amount of detectable $As^V$ produced via HMO oxidation is a function of initial $As^{III}$ concentration with a greater percent of initial $As^{III}$ oxidized at lower concentrations. $As^V$ peak areas converted to concentration (Table S1) for final pH values reveal mean $As^V_{max}$ values of 21.9, 27.3, and 35.3 mmol $kg^{-1}$ from initial $As^{III}$ concentrations of 25, 50, and 75 mmol $kg^{-1}$, respectively. The initial slope, which represents the rapid initial reaction, for $As^{III}$ oxidation does not change substantially under the various reaction conditions with $m_{30s}$ ranging from 0.07 to 0.15 for HMO and from 0.17 to 0.25 for birnessite (Table 1).

$As^V$ remains bound to HMO at pH 6 and 9 following washing with both NaCl and $CaCl_2$ (Fig. 6). Comparison of filtered HMO-As (mineral paste) with washed HMO-As shows some desorption of $As^V$, particularly at pH 6 (greater desorption with $CaCl_2$). At pH 9 a peak shift 860 $cm^{-1}$ to 867 and 873 $cm^{-1}$ upon washing with $CaCl_2$ and NaCl, respectively, is observed. Also at pH 9 a peak at 906 $cm^{-1}$ is present in spectra for the HMO-As slurry, filtered HMO-As, and the HMO-As filtrate.

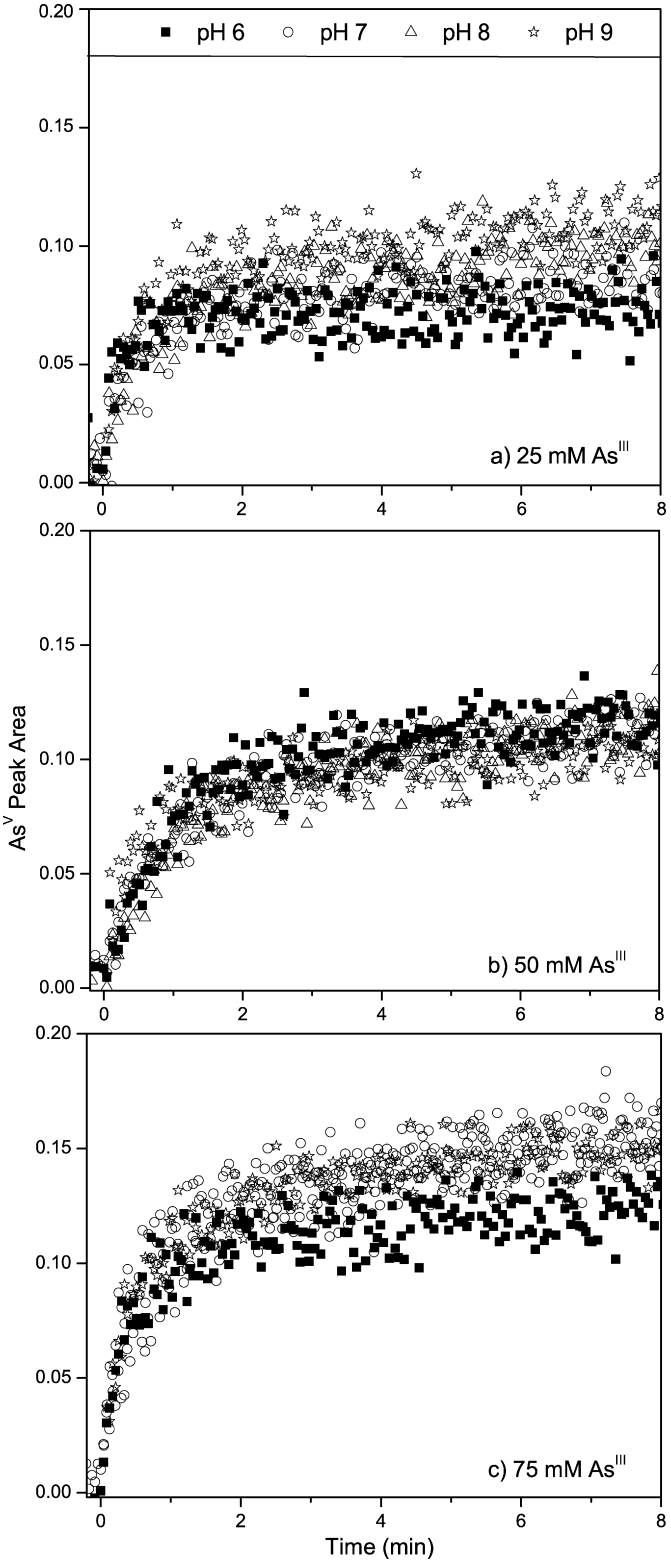


Fig. 5. *In situ* ATR-FTIR kinetic measurements showing $As^V$ production via oxidation of (a) 25 mmol $kg^{-1}$ $As^{III}$, (b) 50 mmol $kg^{-1}$ $As^{III}$, and (c) 75 mmol $kg^{-1}$ $As^{III}$ via HMO at pH 6, 7, 8, and 9.

This peak is absent from the spectra of washed samples. At pH 6 small peaks around 800 $cm^{-1}$ are present for spectra of both NaCl and $CaCl_2$ washed samples.

Table 1
$As^{III}$ oxidation rate parameters for HMO and birnessite representing averaged $As^{V}_{max}$ with standard deviation[a], time to reach half $As^{V}_{max}$ ($t_{1/2}$), slope of initial 30 s of reaction ($m_{30\,s}$), and corresponding $R^2$

| | $As^{III}$ oxidation by HMO | | | | | | | | | | | |
|---|---|---|---|---|---|---|---|---|---|---|---|---|
| pH | 6.0 | | | 7.0 | | | 8.0 | | | 9.0 | | |
| $[As^{III}]^b$ | 25 | 50 | 75 | 25 | 50 | 75 | 25 | 50 | 75 | 25 | 50 | 75 |
| $[As^{V}_{max}]^b$ | 22.5 (3.00) | 34.2 (2.56) | 38.0 (3.25) | 19.2 (2.11) | 25.3 (2.03) | 35.9 (3.24) | 24.1 (2.25) | 26.3 (2.13) | 36.8 (2.89) | 21.9 (1.99) | 23.2 (2.45) | 30.3 (1.91) |
| $t_{1/2}$ (min) | 0.21 | 0.91 | 0.31 | 0.44 | 0.63 | 0.69 | 0.46 | 0.80 | 0.35 | 0.32 | 0.37 | 0.35 |
| $m_{30\,s}$ | 0.09 | 0.07 | 0.15 | 0.07 | 0.09 | 0.09 | 0.09 | 0.07 | 0.14 | 0.11 | 0.14 | 0.14 |
| $R^2$ | 0.68 | 0.69 | 0.86 | 0.49 | 0.82 | 0.79 | 0.64 | 0.76 | 0.75 | 0.81 | 0.74 | 0.84 |
| | $As^{III}$ oxidation by birnessite | | | | | | | | | | | |
| pH | 6.0 | | | | | | 9.0 | | | | | |
| $[As^{III}]^b$ | 75 | | | | | | 75 | | | | | |
| $[As^{V}_{max}]^b$ | 24.7 (1.93) | | | | | | 22.4 (2.15) | | | | | |
| $t_{1/2}$ (min) | 0.17 | | | | | | 0.26 | | | | | |
| $m_{30\,s}$ | 0.25 | | | | | | 0.17 | | | | | |
| $R^2$ | 0.88 | | | | | | 0.63 | | | | | |

[a] Standard deviation of mean $[As^{V}_{max}]$ values given in parenthesis.
[b] $As^{III}$ and $As^{V}$ concentration in mmol $kg^{-1}$.

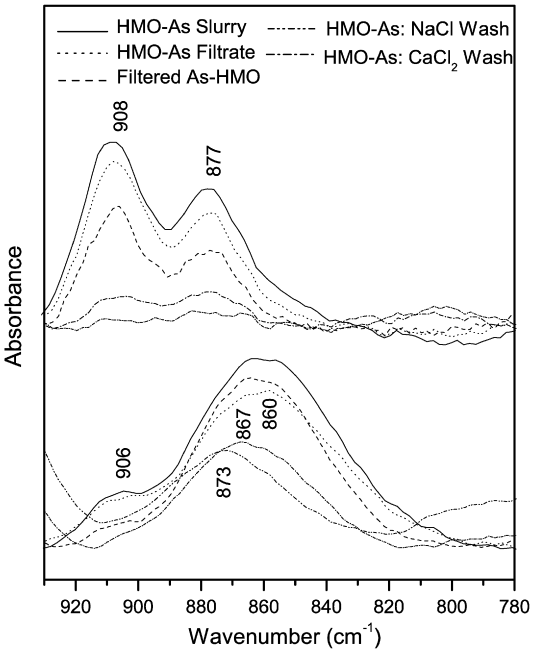


Fig. 6. ATR-FTIR spectra of HMO reactions with 75 mmol $L^{-1}$ $As^{III}$ at pH 6 and 9; (—) represents the As-HMO slurry, (···) is filtrate of the reacted slurry, (- - -) shows spectra of the filtered paste after reaction (not washed), (- · · -) is NaCl washed HMO paste after reaction, and (- · · ·) represent $CaCl_2$ washed HMO pasted after reaction.

### 3.3. In situ flow experiments

$As^{III}$ (75 mmol $kg^{-1}$) entering the flow chamber is rapidly oxidized upon encountering HMO surfaces, and $As^{V}$ is detected at the IRE interface (Fig. 7). Results at pH 9 reveal $As^{V}$ peaks located at 859 and 900 $cm^{-1}$. The 859 $cm^{-1}$ peak appears prior to the 900 $cm^{-1}$ peak and, while it decreases in intensity after 11.5 min of reaction, remains at the conclusion of the reaction time. The disappearance of the 900 $cm^{-1}$ peak corresponds to the emergence of an $As^{III}$ peak at 794 $cm^{-1}$, indicating decreased $As^{III}$ oxidation. Similar trends are observed for pH 6, except peak production at 859 and 900 $cm^{-1}$ is simultaneous and the 900 $cm^{-1}$ peak also remains at the end of the reaction time. Measurement of effluent pH reveals a pH change from 9 to 8.7 and from 6 to 5.8 over the course of the experiments. The $As^{V}_{max}$ (11.5 min) for flow experiments with a 75 mmol $kg^{-1}$ $As^{III}$ solution, at a flow rate of 20 μL $min^{-1}$, is 39.9 mmol $kg^{-1}$ at pH 9 and 31.5 mmol $kg^{-1}$ at pH 6.

## 4. Discussion

### 4.1. Rapid-scan ATR-FTIR for monitoring initial reaction kinetics

The rapid-scan FTIR method presented in this study permits evaluation of initial reaction rates at the solid–liquid interface. The data demonstrate successful use of the technique to monitor the rapid reaction kinetics of an IR active compound at the mineral/water interface. Under the conditions of this study, rapid $As^{III}$ oxidation was observed via both a relatively amorphous Mn oxide (HMO) and a more crystalline Mn-oxide (birnessite) using both static and flow techniques. Both solution-phase and bound $As^{V}$ are detected and spectra reflect the total amount of $As^{V}$ produced. This method does not require separation of the solid and solution phase, nor extraction from the Mn-oxide, to detect total $As^{V}$ produced and therefore sorption/desorption of $As^{V}$ with the mineral surface does not influence the observed reaction rates. The results demonstrate a series of rapid reactions leading to $As^{III}$ oxidation, where transport is limited, that are independent of reactant concentration and primarily chemically controlled [4].

### 4.2. Rapid $As^{III}$ oxidation: static experiments

In the current study, a high solid to solution ratio was used to create a Mn-oxide slurry for reactions. The Mn-oxide sus-

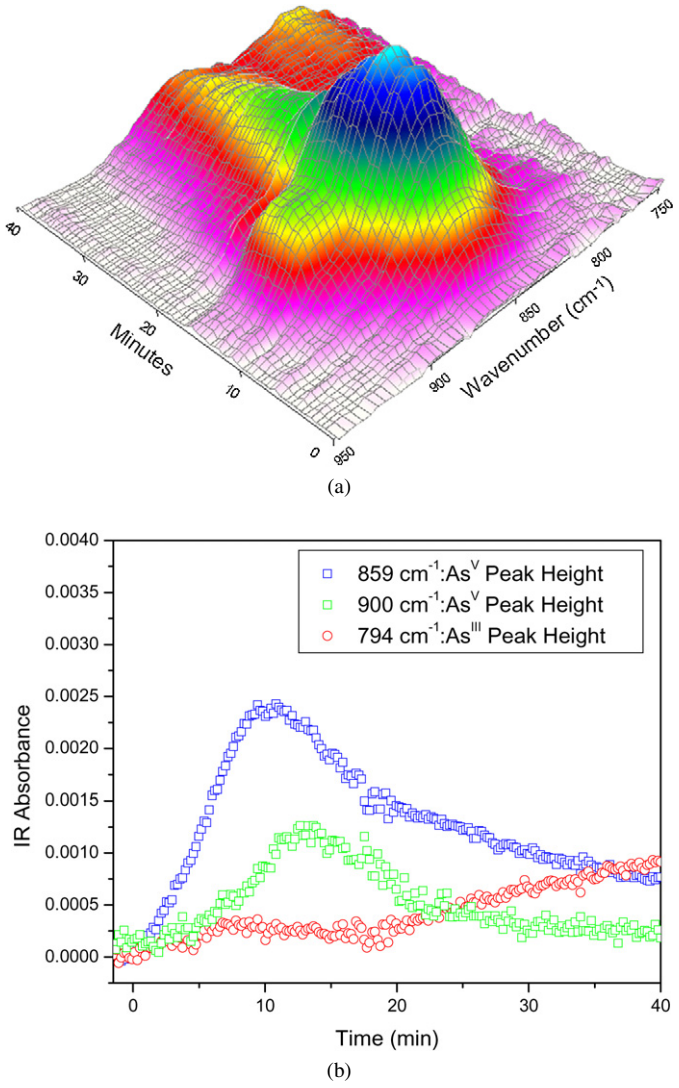


Fig. 7. *In situ* flow FTIR data for 75 mmol $kg^{-1}$ $As^{III}$ oxidation via HMO at pH 9 showing (a) all IR spectra over the course of the reaction; transition from pink to yellow to green to blue indicate increasing IR absorbance ($Y$-axis). And, (b) the IR absorbance of peaks corresponding to $As^{III}$ (794 $cm^{-1}$) and $As^{V}$ (859 and 900 $cm^{-1}$). (For interpretation of the references to color in this figure legend, the reader is referred to the web version of this article.)

pension was added to an equal volume of $As^{III}$ solution, permitting instantaneous mixing and preventing preferential $As^{V}$–Mn-oxide accumulation at the IRE-water interface (Fig. 2). While both HMO and $As^{III}$ concentrations are much higher than previous studies, the Mn:As ratio is within the same order of magnitude [13]. Because of IR detection limits, concentrations of $As^{III}$ used in this study are higher than typically found in the environment. The reproducibility of data collected using various mixing and settling approaches is attributed to the homogeneous slurry of HMO-As at the IRE interface extending beyond the IR beam depth of penetration (Fig. 2).

Under the experimental parameters (pH 6, 7, 8, 9; $[As^{III}]$ = 25, 50, 75 mmol $kg^{-1}$) rapid initial $As^{III}$ oxidation is observed regardless of the type of Mn-oxide (Fig. 4), As concentration, or pH (Fig. 5). The lack of pH dependence on the $As^{III}$ oxidation rate by a synthetic birnessite (pH 5 to 8.2) has been documented [13]. Although the oxidation of $As^{III}$ via Mn-oxides consumes protons, the binding of $As^{III}$ and $Mn^{II}$ displaces protons from the hydroxylated mineral surface to solution [13] and can lower the reaction pH. The high solid to solution ratio used in this study, with extensive $As^{III}$ oxidation, results in a high number of protons released from the surface, and may explain the observed decrease in reaction pH.

Under the current experimental conditions the reaction proceeds rapidly and is apparently shut down due to high concentration of reaction products which are rapidly produced. The reaction products, $As^{V}$ and $Mn^{II}$, may bind to the HMO surface or possibly precipitate onto the surface (e.g., krauite) [22]. Desorption experiments of batch $As^{III}$-HMO reactions confirm binding of $As^{V}$ at both pH 6 and 9. Increased desorption of $As^{V}$ with $CaCl_2$ at pH 6 (compared to NaCl) suggests exchange of $Ca^{II}$ for $Mn^{II}$ leading to increased $As^{V}$ release. This is in agreement with previous studies proposing $As^{V}$ binding to Mn-oxide through surface-bound $Mn^{II}$ [11,12]. At pH 9, HMO is more negatively charged and presumably $Mn^{II}$ is held more tightly. Therefore, desorption of both $Mn^{II}$ and $As^{V}$ is similar upon washing with NaCl and $CaCl_2$.

At pH 9, the 860 $cm^{-1}$ peak in spectra of washed samples shifts to higher wavenumbers, indicating a change in the $As^{V}$ [i.e., $\nu_{as}$(As–O)] coordination upon binding to HMO. Similar upshifts in the spectra of mineral pastes for boric acid adsorption to amorphous Al-oxide were attributed to strengthening of O–B and B–OH bonds when boric acid is complexed with the mineral surface [23]. Washing of pH 9 samples also results in the disappearance of the 906 $cm^{-1}$ peak. This peak likely represents a degree of $As^{V}$ protonation resulting from the reaction pH approaching the second p$K_a$ (7.94) [24]. The absence of this peak for bound $As^{V}$ indicates preferential/stronger sorption of the more hydroxylated species.

The apparent time for $As^{III}$ depletion is less than has been observed in previous studies investigating $As^{III}$ oxidation via Mn-oxides, with $t_{1/2}$ calculated from initial $As^{III}$ depletion (oxidation and sorption) rate constants ranging from 0.15 to 34.7 h [13,22]. The $As^{III}$ oxidation data collected using the rapid-scan FTIR technique provides data for a rapid initial reaction that is not observed in previous studies, however the common hypothesis of a multiprocess mechanism involving $As^{III}$ sorption, $As^{III}$ oxidation, $Mn^{IV}$ reduction (to $Mn^{III}$ and $Mn^{II}$), and subsequent sorption of $As^{V}$ and $Mn^{II}$ [13,25] is not disputed. Ongoing work in our lab using *ex situ* batch to study $As^{III}$ oxidation by HMO (filtered solution $As^{III}$ and $As^{V}$ measured by ICP-AES) reveal $As^{V}_{max}$ is reached on a time scale of hours (Fig. S1) rather than sec to min, as shown by the rapid-scan FTIR results in the current study. The data in this study demonstrate that a large portion of chemical reactions can occur within the first few minutes of reactions; reaffirming our belief that rapid data acquisition (timescale of sec) is required to observe initial reaction rates. We are not disagreeing with reported reaction rates, but are rather bringing attention to the initial reaction which is missed in previous work.

### 4.3. Rapid $As^{III}$ oxidation: flow experiments

The continuous input of $As^{III}$ to the HMO within the flow cell, and subsequent removal of effluent solution, results in increased time for the reaction to approach completion ($t_{1/2}$ = 5.1 min) and the presence of $As^{III}$ at the crystal interface at about 5 min followed by increased $As^{III}$ peak absorbance after 20 min of reaction (Fig. 7). In this reaction, $As^{III}$ is directly oxidized by the Mn-oxide via a surface mechanism and $Mn^{II}$ and $As^{V}$ are released to solution [25,26]. The oxidation of $As^{III}$ by Mn-oxides can be a self inhibiting process due to sorption of $As^{V}$ and $Mn^{II}$, which coat the oxide surface, prohibiting interaction between $MnO_2$ and $As^{III}$ [25,26]. The removal of these reaction products by the effluent solution likely reduces sorption of $As^{V}$ and $Mn^{II}$ to HMO; therefore, surface sites for $As^{III}$ oxidation are available for a longer time period.

During flow experiments the production of an IR peak at 900 $cm^{-1}$ (Fig. 7) is observed during $As^{III}$ oxidation via HMO at pH 9. This peak appears slightly after the emergence of the 859 $cm^{-1}$ peak, its intensity grows at a slower rate, and its reduction corresponds almost exactly with the decreased intensity of the 900 $cm^{-1}$ peak. This peak is unexpected as the pH remains relatively unchanged. $As^{V}$ has $pK_{a1}$, $pK_{a2}$, and $pK_{a3}$ values of 2.24, 7.94, and 12.19, respectively [24]. At pH 9, $HAsO_4^{2-}$ predominates and a peak at 908 $cm^{-1}$ is not observed (Fig. 1b). This peak is typically observed at pH values below the $pK_{a2}$ (pH 7.95) and is therefore attributed to either a localized reduction of pH at the liquid–mineral interface or to sorption induced protonation upon binding of $As^{V}$ to the Mn-oxide through surface OH groups or via water bridging. At this pH HMO surfaces are also mostly deprotonated, however during reductive mineral dissolution the release of $Mn^{II}$ from the mineral surface can result in protonation of Mn-O groups at the surface [13]. Similarly, a FTIR peak assigned to COOH at pH 7 ($pK_a < 5$) was observed upon bacterial adhesion to hematite [9]. This mechanism may also contribute to the observed peak at 908 $cm^{-1}$ for static $As^{III}$ reaction with HMO (Figs. 2 and 6), however since a pH change is observed (pH 9 to 7.5) the peak is predicted. A similar peak at 908 $cm^{-1}$ was observed for $As^{V}$ sorption to birnessite and HMO (Fig. 1b). At the conclusion of the flow experiments the peak at 856 $cm^{-1}$ remains and is attributed to $As^{V}$ on the HMO surface, perhaps due to production of an $As^{V}$–Mn phase [25,27]. These data demonstrate that retention of $As^{V}$ to Mn-oxides does occur, and that understanding the mechanism of sorption is very important as this will greatly affect its fate and transport in soils and subsurface environments.

## 5. Summary

The unique approach of this study permits examination of $As^{III}$ oxidation kinetics of IR active compounds at the Mn-oxide–liquid interface, thus permitting examination of initial reaction kinetics while simultaneously providing molecular-scale data. Data collected under both static and flow conditions can be used to study the rapid initial reaction and elucidate mechanisms under various environmental conditions. We have demonstrated that initial $As^{III}$ oxidation via Mn-oxides occurs more rapidly than previously reported; due to different methodologies and the previous inability to measure rapid reactions. Additionally, $As^{V}$ sorption to Mn-oxides subsequent to $As^{III}$ oxidation likely occurs through surface-bound $Mn^{II}$. Exchange of $Mn^{II}$ with cations (e.g., $Na^{+}$, $Ca^{2+}$) results in some desorption of $As^{V}$, and will greatly influence the environmental transport of arsenic in the presence of high Mn-oxide concentrations. Study of the As-Mn system is ongoing, particularly to determine reaction mechanisms, including analysis of solution phase As and Mn species via FTIR and additional analytical techniques. As illustrated through examination of Mn-oxide catalyzed $As^{III}$ oxidation, rapid-scan ATR-FTIR spectroscopy has great potential for exploring rapid kinetic reactions for a myriad of organic and inorganic reactions occurring at the solid–liquid interface.

## Acknowledgments

We thank Michael J. Borda for assistance with the synthesis of HMO and helpful discussions at the early stages of this research. We also thank the laboratory of Jon Chorover for donation of birnessite. Zhenqing Shi, Matthew Ginder-Vogel, and Aaron Thompson provided helpful insights and discussions during preparation of this manuscript. This project was supported by the National Research Initiative of the USDA Cooperative State Research, Education and Extension Service, grant number 2005-35107-16105 and the National Science Foundation, grant number EAR-0544246.

## Supplementary information

Supplementary information for this article may be found on ScienceDirect, in the online version.

Please visit DOI: 10.1016/j.jcis.2007.12.017.

## References

[1] M.C. Amacher, in: D.L. Sparks, D.L. Suarez (Eds.), Rates of Soil Chemical Processes, Soil Sci. Soc. Am., Madison, WI, 1991, p. 19.
[2] A.M. Scheidegger, D.L. Sparks, Soil Sci. 161 (1996) 813.
[3] C.J. Matocha, A.D. Karathanasis, S. Rakshit, K.M. Wagner, J. Environ. Qual. 34 (2005) 1539.
[4] D.L. Sparks, Kinetics of Soil Chemical Processes, Academic Press, San Diego, 1989.
[5] K.F. Hayes, J.O. Leckie, in: J.A. Davis, K.F. Hayes (Eds.), Geochemical Procces at Mineral Surfaces, Am. Chem. Soc., Washington, DC, 1986, p. 114.
[6] S. Mitsunobu, Y. Takahashi, T. Uruga, Anal. Chem. 78 (2006) 7040.
[7] A. Voegelin, S.J. Hug, Environ. Sci. Technol. 37 (2003) 972.
[8] M.I. Tejedor-Tejedor, M.A. Anderson, Langmuir 6 (1990) 602.
[9] S.J. Parikh, J. Chorover, Langmuir 22 (2006) 8492.
[10] I.V. Chernyshova, J. Electroanal. Chem. 558 (2003) 83.
[11] D.W. Oscarson, P.M. Huang, W.K. Liaw, U.T. Hammer, Soil Sci. Soc. Am. J. 47 (1983) 644.
[12] Y. Tani, N. Miyata, M. Ohashi, T. Ohnuki, H. Seyama, K. Iwahori, M. Soma, Environ. Sci. Technol. 38 (2004) 6618.
[13] M.J. Scott, J.J. Morgan, Environ. Sci. Technol. 29 (1995) 1898.
[14] J.J. Morgan, W. Stumm, J. Colloid Sci. 19 (1964) 347.

[15] R.R. Gadde, H.A. Laitlinen, Anal. Chem. 46 (1974) 2022.
[16] J.W. Murray, J. Colloid Interface Sci. 46 (1974) 357.
[17] R.M. McKenzie, Mineral. Mag. 38 (1971) 493.
[18] J. Chorover, M.K. Amistadi, Geochim. Cosmochim. Acta 65 (2001) 95.
[19] G. Sposito, The Chemistry of Soils, Oxford Univ. Press, New York, 1989.
[20] A.J. Roddick-Lanzilotta, A.J. McQuillan, D. Craw, Appl. Geochem. 17 (2002) 445.
[21] S. Goldberg, C.T. Johnston, J. Colloid Interface Sci. 234 (2001) 204.
[22] C. Tournassat, L. Charlet, D. Bosbach, A. Manceau, Environ. Sci. Technol. 36 (2002) 493.
[23] S. Goldberg, C. Su, in: F. Xu, H.E. Goldbach, P.H. Brown, R.W. Bell, T. Fujiwara, C.D. Hunt, S. Goldberg, L. Shi (Eds.), Advances in Plant and Animal Boron Nutrition, Springer, Netherlands, 2007, p. 313.
[24] W.P. Inskeep, T.R. McDermott, S. Fendorf, in: W.T. Frankenberger Jr. (Ed.), Environmental Chemistry of Arsenic, Marcel Dekker, New York, 2002, p. 183.
[25] B.A. Manning, S.E. Fendorf, B. Bostick, D.L. Suarez, Environ. Sci. Technol. 36 (2002) 976.
[26] D.W. Oscarson, P.M. Huang, W.K. Liaw, Clays Clay Miner. 29 (1981) 219.
[27] J.N. Moore, J.R. Walker, T.H. Hayes, Clays Clay Miner. 38 (1990) 549.